Journal of Nuclear and Radiochemical Sciences, Vol. 15, No.1, pp. 7-13, 2015

Articles

Evaluation of a new sector-field ICP-MS with Jet Interface for ultra-trace determination of Pu isotopes: from femtogram to attogram levels

J. Zheng*

Research Center for Radiation Protection, National Institute of Radiological Sciences, Anagawa 4-9-1, Inage, Chiba 263-8555, Japan

Received February 19, 2015; Received in revised form April 27, 2015; Accepted May 12, 2015

In March 2014, a new sector-field (SF)-ICP-MS (Element XR) equipped with the Jet Interface was installed in the Research Center for Radiation Protection at the National Institute of Radiological Sciences (NIRS). This is the first Element XR installed for actinides measurements in Japan. In this paper, a detail evaluation is made of the Element XR on its analytical potential for ultra-trace determination of Pu isotopes. In order to enhance the sensitivity for Pu isotope analysis, high efficiency sample introduction systems (APEX-Q and Aridus II) were combined with the Element XR. A certified Pu isotope standard solution (NBS 947) and a multi element standard solution (Merck Multi Element Standard), which contained depleted U, were used to investigate four items: the formation rate of $^{238}UH^+$, which could interfere with an ultra-trace level ^{239}Pu determination; the detection limit for Pu; the precision and accuracy for $^{240}Pu/^{239}Pu$ atom ratio measurement; and the long-term (8- month) stability for Pu isotope composition analysis. Due to the exceptionally high sensitivity of the new SF-ICP-MS, a detection limit at the attogram (10^{-18} g) level was achieved. This is comparable to or even surpasses the detection limit of accelerator mass spectrometry, which has long been regarded as the most sensitive technique for Pu isotope measurement.

1. Introduction

Essentially all of the Pu found in the environment is of anthropogenic origin, and it is a product of human activities (such as atmospheric nuclear weapons testing, reprocessing of nuclear fuel, and releases from nuclear accidents) of the past seven decades, although trace amounts of ^{239}Pu and ^{244}Pu are present naturally either from a primordial Earth origin or from neutron capture by ^{238}U [1-4]. Due to the high radiological toxicities and very long radioactive half-lives, Pu isotopes are regarded as highly hazardous contaminants in the environment, and the most frequently monitored Pu isotopes are ^{238}Pu, ^{239}Pu, ^{240}Pu and ^{241}Pu with half-lives of 87.7 y, 24110 y, 6561 y and 14.4 y, respectively [5]. The isotopes ^{238}Pu, ^{239}Pu, and ^{240}Pu all decay by emission of α particles, while ^{241}Pu undergoes β decay to produce ^{241}Am. It was well-known that Pu isotopic compositions ($^{238}Pu/^{239+240}Pu$ activity ratio, $^{240}Pu/^{239}Pu$ atom ratio and $^{241}Pu/^{239}Pu$ atom ratio) vary significantly in the environment depending on the emission source [6], the Pu isotopic ratio, therefore, has been used as a fingerprint for contamination source identification. Although $^{238}Pu/^{239+240}Pu$ activity ratio has been used for contamination identification for a long-time, its measurement with alpha spectrometry is time consuming. With the development of ICP-MS technique, rapid determination of $^{240}Pu/^{239}Pu$ and $^{241}Pu/^{239}Pu$ atom ratios is achievable. Thus, the use of atom ratios of $^{240}Pu/^{239}Pu$ and $^{241}Pu/^{239}Pu$ has been found wider applications for contamination source identification. For example, the atom ratio of $^{240}Pu/^{239}Pu$ allows weapons-grade Pu (0.01-0.05) to be distinguished from reprocessing Pu (0.2-0.8) and global fallout Pu (0.17-0.19), and the transport of Pu from different sources to be studied [7].

In recent years, there has been an increasing demand for ultra-trace determination of Pu isotopes in studies on radiation protection [8], safeguards and nuclear forensics [9,10], and environmental studies, such as tracing the sources of radioactive contamination, revealing the transport process of aerosols in the atmosphere, establishing new geochronology [11,12], and in investigating ongoing environmental changes, for instance, soil erosion and desertification [13-15]. Conventionally, alpha spectrometry has usually been used for Pu measurement in various environmental samples. This method, however, normally requires a tedious chemical separation procedure and long counting times (days to weeks). Moreover, alpha spectrometry cannot distinguish ^{239}Pu and ^{240}Pu due to the closeness of the alpha radiation energies (5.16 MeV and 5.17 MeV for ^{239}Pu and ^{240}Pu, respectively), so it cannot provide isotopic composition information. In contrast, mass spectrometry, especially ICP-MS, as an atom-counting approach that counts the atoms themselves, irrespective of their decay mode, specific activity, or half-life, is gradually replacing alpha spectrometry as a main-stream technique for Pu isotopic analysis. Due to the strength of the argon plasma source used for ICP-MS, almost 100% ionization efficiency can be achieved for Pu isotopes with the first ionization potential of 6.03 eV as calculated from the Saha equation, thus, highly sensitive determination of Pu isotopes can be realized. Recent development of ICP-MS techniques, especially sector-field (SF)-ICP-MS, has pushed the detection limit for analysis of Pu isotopes down to the sub-femtogram level [16-19].

A new SF-ICP-MS, Element XR equipped with the Jet Interface was installed in the Research Center for Radiation Protection at the National Institute of Radiological Sciences (NIRS) in March 2014. As this Element XR is the first in Japan to be installed for actinide analysis, a detailed investigation was made on its analytical potential for Pu isotopes. In combination with the high efficiency sample introduction systems (APEX-Q and Aridus II), an exceptionally high sensitivity was obtained, and a detection limit at the attogram (10^{-18} g) level was achieved, which is comparable to or even better than the detection limit of accelerator mass spectrometry (AMS).

2. Experimental

2.1. Explanation and features of the Element XR. The Element XR (Thermo Scientific, Bremen, Germany) was devel-

*Corresponding author. E-mail: jzheng@nirs.go.jp Tel: 81-043-206-4634 Fax: 81-043-255-0721

Published on Web 06/04/2015

oped from the Element 2 by introducing a high efficient sample interface, the Jet Interface, to further improve the sensitivity. Thus, like the Element 2, the Element XR is a high performance, double-focusing magnetic SF-ICP-MS with the capability for rapid multi-element and isotopic ratio measurements. The important instrumental characteristics of the Element XR can be briefly summarized as follows [20].

(1) Plasma ion source and interface: the argon plasma ion source and sampling interface of the Element XR are at ground potential, which reduces the initial kinetic energy spread, thus increasing the ion transmission and delivering high sensitivity at all resolutions. The Jet Interface, which consists of a high capacity dry interface pump and the Jet sampler cone, further increases the sensitivity required for long-lived radionuclides analysis.

(2) Detection system: the Element XR has a discrete dynode detector system, so the ion beam does not have to directly strike the detector to initiate an electron cascade. The secondary electron multiplier uses a conversion dynode at -8 kV, producing a uniform response across the mass range. By incorporating a single Faraday detector, the detection system of the Element XR raises the linear dynamic range to $>10^{12}$ orders of magnitude, thus trace and major elements can be quantified in a single analysis.

2.2. Outline of the high efficiency sample introduction systems: APEX-Q and Aridus II. Figure 1 shows schematic diagrams of the SF-ICP-MS (Element XR) coupled to the high efficiency sample introduction systems (APEX-Q and Aridus II) and Table 1 lists some of the instrument and data acquisition settings.

The APEX-Q is a desolvation sample introduction system (Element Scientific Inc., USA) for ICP to enhance sensitivity and lower formation of H_2O-origin background species, such as UO^+ and uranium hydrides (UH^+ and UH_2^+) which can interfere with ^{239}Pu and ^{240}Pu determination. A nebulizer sprays the sample mist at 100 °C into a heated cyclonic spray chamber, the mist is subsequently cooled with a peltier-cooled multipass condenser to 2 °C , and then it is transported to the desolvation membrane module (ACM Nafion fluoropolymer membrane desolvation module). A countercurrent flow of Ar sweep gas is introduced to remove solvent vapors that permeate the membrane wall. Nonvolatile sample components do not pass through the membrane wall; instead they continue to the SF-ICP-MS torch injector where they are ionized in the plasma. Thus, only dry aerosol particles are loaded to the plasma. This system can be used with different nebulizers that provide a wide range of sample uptake rates from 20 μL min^{-1} to over 1 mL min^{-1}. The nebulizers can be either self-aspirated or pumped. Because the spray chamber is heated to 140 °C and the condenser is at 2 °C, the generated aerosols are uniform and have only a small amount of moisture. The improved sensitivity of the APEX-Q is due to the increase of both the sample transport efficiency and the aerosol quality. Further sensitivity

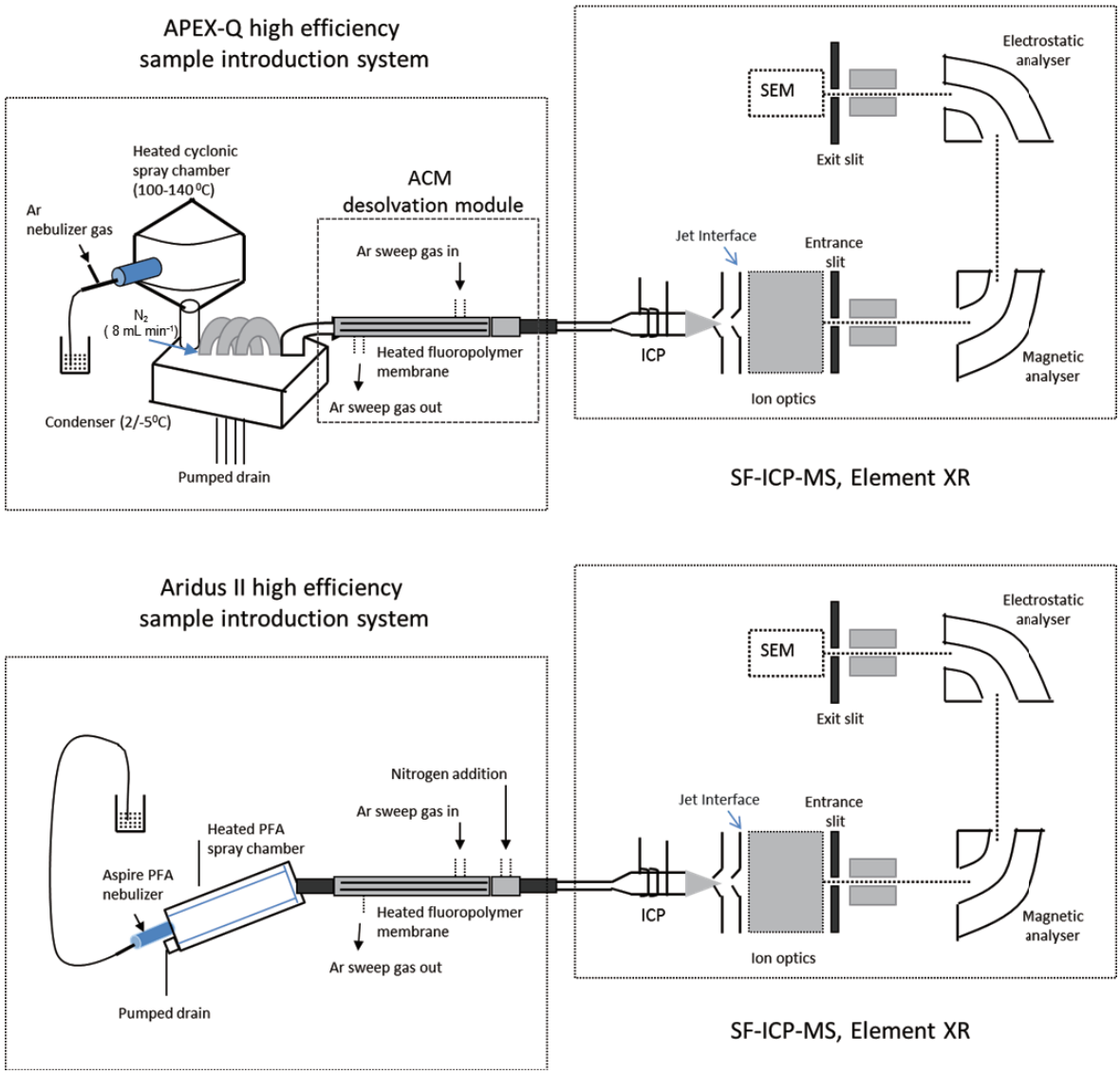

Figure 1. Schematic diagrams of the SF-ICP-MS (Element XR) coupled to the APEX-Q and Aridus II sample introduction systems.

TABLE 1: Instrument and data acquisition settings for SF-ICP-MS (Element XR) and the sample introduction systems (APEX-Q and Aridus II)

SF-ICP-MS	
Instrument settings	
Forward power	1200 W
Nebulizer	Conical concentric and PFA Aspire
Sample cone	Nickel, 1.1 mm orifice diameter
Skimmer cone	Nickel, 0.8 mm orifice diameter or X-cone with Jet Interface
Torch	Fassel
Cool gas	16 L min^{-1}
Auxiliary gas	0.85 L min^{-1}
Sample gas (nebulizer gas)	0.97-1.00 L min^{-1} (optimized daily to highest intensity of $^{238}U^{+}$ and lowest possible oxide formation rate)
Data acquisition settings	
Low resolution (m/Δm = 300):	
Acquisition mode	E-scan (peak jumping)
Monitored mass (*m/z*)	238, 239, 240, 241, 242
No. of scans (runs x passes)	20 × 4
Mass window	10 %
Samples per peak	100
Sample time	10 ms for $^{238}U^{+}$; 30 ms for $^{242}Pu^{+}$; 70 ms for $^{239}Pu^{+}$; and 100 ms for $^{240}Pu^{+}$ and $^{241}Pu^{+}$
Integration type	Average
Total time of analysis	150 s
APEX-Q settings	
Sample uptake rate	0.2 mL min^{-1} (with conical nebulizer)
Spray chamber temperature	140 °C
Condenser temperature	2 °C
Sweep gas (Ar)	3 L min^{-1}
Additional gas (Ar)	0.1 L min^{-1}
N_2 gas	8~10 mL min^{-1}
Aridus II settings	
Sample uptake rate	0.05 mL min^{-1} (with PFA Aspire nebulizer)
Spray chamber temperature	110 °C
Membrane oven temperature	160 °C
Sweep gas (Ar)	6.5 L min^{-1}
N_2 gas	~ 5 mL min^{-1}

improvement can be gotten by introducing N_2 gas into the APEX-Q. For Pu analysis, the sensitivity enhancement was not due to the effect of charge transfer with Pu atom resulting in ionization of Pu. Considering the quite low first ionization potential of Pu (6.03 eV), Pu tends to be almost completely ionized in the hot plasma, the sensitivity improvement is most likely a result of minimizing PuO formation [21]. For cleanup after use, the ACM desolvation module is easily removed from the APEX, and cleaned using an acidic solution.

The Aridus II desolvation system is also widely used for ultra-trace radionuclide measurement. It consists of a self-aspiration nebulizer, the Aspire PFA nebulizer, equipped on the heated PFA spray chamber which is connected to column with the heated fluoropolymer membrane. The nebulizer sprays sample solution into the heated PFA spray chamber; the high temperature (up to 110 °C) maintains the sample in the vapor phase. The sample vapor then enters the heated PTFE membrane desolvator module. Similar to the APEX-Q system, a countercurrent flow of Ar sweep gas is introduced to remove solvent vapors that permeate the membrane wall. Nonvolatile sample components do not pass through the membrane wall; instead they continue to the SF-ICP-MS torch injector where they are ionized in the plasma. The difference between the APEX-Q and the Aridus II is that in the latter, the sample mist from the heated spray chamber is immediately transported to the membrane desolvation module without passing through a condenser to cool it down. The desolvation module can be easily removed for cleaning. Three different nebulizers can be used to achieve sample uptake rates of 50, 100, or 200 μL min^{-1}.

2.3. Analytical procedure for determination of Pu isotopes in sediment and seaweed reference materials. Two reference materials, NIST-4357 (ocean sediment) and IAEA-446 (seaweed), were used to test the applicability of the new SF-ICP-MS for the determination of Pu isotopes in environmental samples. For NIST- 4357, *ca*. 0.5 g ashed (450 °C, 4 h) samples were digested with HNO_3-HF after adding 0.57 pg ^{242}Pu tracer. The samples were then evaporated to dryness, followed by adding 3 mL $HClO_4$. Next, 3 mL conc. HNO_3 was added and the solution was evaporated to dryness, this step was repeated twice. The residue was dissolved in 50 mL 1 M HNO_3, and 4 mg Fe^{3+} was added as carrier. Then, 2.5 mL $NH_2OH{\cdot}HCl$ (80 g L^{-1}) was added to change Pu to Pu(III) and Pu was further co-precipitated with $Fe(OH)_3$. The precipitate was dissolved in 1.5 mL conc. HNO_3 and then 50 mL 8 M HNO_3 was added to the solution along with 0.4 g $NaNO_2$ to adjust oxidation state of Pu to Pu (IV). For IAEA-446, a nitric acid leaching method was used to release Pu. In brief, 3-8 g seaweed samples were ashed at 450 °C for 4 h, then, samples were transferred to a capped 120 mL Teflon vessel. After adding 20 mL conc. HNO_3, samples were digested at 160˚C for 4 h. After filtration and adjusting the acidity to 8 M HNO_3, 0.41g $NaNO_2$ was added to take Pu to the tetravalent state. After acid leaching or digestion, samples were subject to the subsequent two-stage anion chromatographic chemical separation as described by Bu et al. [22]. Briefly, Pu was separated from sample matrix using an AG 1X8 anion-exchange column. The obtained Pu fraction was further purified using an AG MP-1 M anion-exchange column with HBr for Pu elution. After removing any trace of HBr, the sample was finally dis-

solved in 4% HNO_3 in preparation for the SF-ICP-MS analysis. For Pu isotope ratio measurements, a Pu isotopic standard (NBS 947) was used with sample-standard bracketing to correct externally for instrumental mass bias. Details of the mass bias correction have been described in previous work [18].

3. Results and Discussion

In the present evaluation study on determination of Pu isotopes, the SF-ICP-MS (Element XR) equipped with the Jet Interface was used in the low resolution mode in order to utilize the maximum instrument sensitivity. Additionally, the normal skimmer cone was replaced by a high-efficiency cone (X-cone, Thermo Scientific) for further increasing sensitivity of the SF-ICP-MS. All the measurements were made in the self-aspirating mode to reduce the risk of contamination by the peristaltic pump tubing. The SF-ICP-MS was optimized daily using a 0.1 ng mL^{-1} U standard solution (Merck multi element standard) when using the standard sample introduction system consisting of a concentric nebulizer (50 μL min^{-1} sample uptake) and a Scott-type double-pass spray chamber, and 0.02 ng mL^{-1} U standard solution when using the high efficiency sample introduction systems (APEX-Q and Aridus II). Optimized instrument conditions for the determination of Pu isotopes are listed in Table 1.

3.1. Sensitivity and detection limit for Pu analysis. Figure 2 compares the background levels (cps) in the Pu isotope mass region (*m/z* 238-242) using the APEX-Q and Aridus II sample introduction systems. Diluted nitric acid (4%) was analyzed for this background evaluation. Both systems had similarly low background (*ca*. 2 cps) in the Pu isotope mass region. For these two sample introduction systems, the sensitivity of Pu analysis was estimated using the Pu isotope standard solution (NBS 947) at concentrations of 10 and 100 fg mL^{-1}. The obtained mass spectra are shown in Figure 3. For the Element XR SF-ICP-MS without the Jet Interface (Figure 3A), the signal intensity of 100 fg mL^{-1} ^{239}Pu was *ca*. 350 cps; significant sensitivity improvement was obtained both for the Aridus II/SF-ICP-MS (with Jet Interface) (Figure 3B) and APEX-Q/SF-ICP-MS (with Jet Interface) (Figure 3C). For 100 fg mL^{-1} ^{239}Pu, the signal intensity obtained with the Aridus II/SF-ICP-MS was 10,000 cps, corresponding to a sensitivity of 100 Mcps/ppb (ppb = ng mL^{-1}). For 10 fg mL^{-1} ^{239}Pu, the signal intensity obtained with the APEX-Q/SF-ICP-MS was 600 cps, corresponding to a sensitivity of 60Mcps/ppb. These results indicated that compared to the SF-ICP-MS without the Jet Interface, the combination of the APEX-Q or Aridus II sample introduction system with Jet Interface resulted in *ca*. 20-, or 30-fold sensitivity improvement. The higher sensitivity of the Aridus II system indicated its better desolvation ability. However, it was observed that washing out of the remaining signals of the APEX-Q system was faster than for the Aridus II. This was probably caused by the buildup of analyte and sample matrix on the inner wall of the heated PFA spray chamber of the Aridus II system, which would cause signal spikes and longer sample washout time.

Since the highest sensitivity was obtained with the Aridus II/SF-ICP-MS (with Jet Interface) system, the detection limit was estimated based on the definition of 3 times the standard deviation of blank (4 % HNO_3). An extremely low detection limit of 0.043 fg mL^{-1} was achieved for Pu isotope analysis. Taking into account the low sample uptake rate (0.05 mL min^{-1}) using the PFA nebulizer and the short time for analysis (150 s) (cf. Table 1), a sample solution of only 0.125 mL would be required for Pu isotope analysis, thus an absolute detection limit of 5 attogram (or 1.3×10^4 atoms) could be calculated. This detection limit was about one order of magnitude lower than the detection limit obtained with the APEX-Q/SF-ICP-MS (Element 2) [18], pushing the detection of Pu isotope from the femtogram down to the attogram levels. So far, AMS has been widely recognized as the technique providing the highest

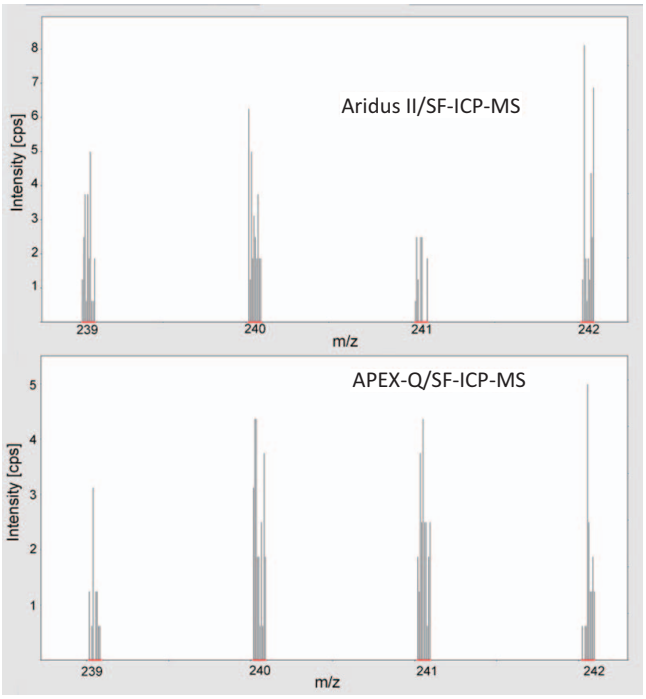

Figure 2. Background levels (cps) of Element XR coupled to the APEX-Q and Aridus II; estimated using 4 % HNO_3.

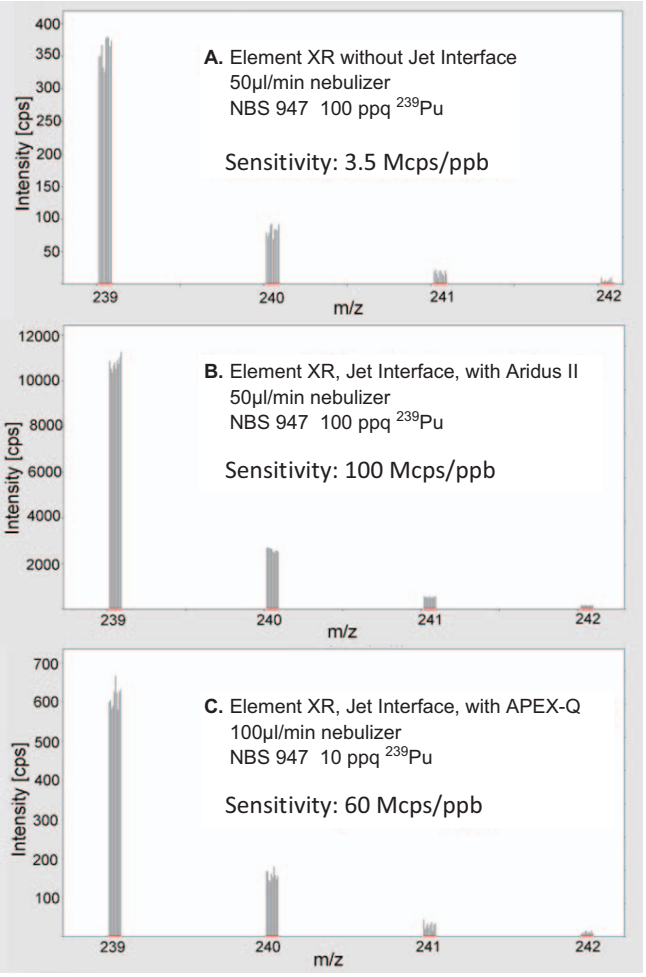

Figure 3. Mass spectra of NBS 947 standard solution obtained using: (A) the Element XR without the Jet Interface; (B) the Aridus II/Element XR with the Jet Interface; and (C) the APEX-Q/Element XR with the Jet Interface.

TABLE 2: Comparison of the interference effect from $^{238}UH^+$ on the determination of ^{239}Pu by SF-ICP-MS with different sample introduction systems

Sample introduction system	UH^+/U^+	References
Pneumatic nebulizer	$7.59 – 8.39 \times 10^{-5}$	27
MCN-100	$4.05 – 4.73 \times 10^{-5}$	27
MicroMist	1.8×10^{-4}	28
Q-DIHEN	$1 – 5 \times 10^{-4}$	28
USN-5000$^+$	$3.20 – 4.00 \times 10^{-5}$	27, 28
USN+MINI-GASS	$2.33 – 2.79 \times 10^{-5}$	27
MCN-6000	$1.35 – 1.80 \times 10^{-5}$	27
Aridus	3.2×10^{-5}	28
APEX-Q with ACM unit	$1.16 – 1.95 \times 10^{-5}$	18
APEX-Q with ACM unit (Element XR-Jet Interface)	2.0×10^{-5}	This study
Aridus II (Element XR-Jet Interface)	2.2×10^{-5}	This study

TABLE 3: Precision and accuracy of ultra-trace Pu isotope analysis using Aridus II/SF-ICP-MS with a single measurement (runs × passes 20 × 4)

Analytical system	$^{240}Pu/^{239}Pu$ atom ratio		^{239}Pu conc. (fg mL^{-1})	Precision (RSD %)	Accuracy (%)
	Measured	Certified			
A	0.234±0.048	0.242	100	20.5	-3.3
B	0.240±0.012	0.242	100	5.0	0.83

A: Element XR without Jet Interface.
B: Aridus II/SF-ICP-MS with Jet Interface.

sensitivity for ultra-trace Pu isotope analysis [23], and the reported detection limit has ranged from 10^4 to 10^6 atoms [23-26]. Therefore, the detection limit obtained with the Aridus II/SF-ICP-MS (with Jet Interface) system is definitely comparable to or even better than the AMS detection limit.

3.2. Effect of UH^+ interference. The presence of uranium in environmental samples may hamper the accurate determination of Pu isotopes, especially for ^{239}Pu, due to uranium hydride ion formation ($^{238}UH^+$) and the peak tailing effect from $^{238}U^+$. The sample introduction system is recognized as the most important factor affecting formation of uranium hydride ions in a plasma compared with other factors, such as gas flow rate, and the distance of the torch from the cone [18]. Then a 0.1 ng mL^{-1} U standard solution was used to evaluate the $^{238}UH^+$ formation rate in the APEX-Q and Aridus II systems and it was ca. 2×10^{-5} (Table 2). This rate was similar to that for the APEX-Q/Element 2 system [18], indicating that the Jet interface equipped in the Element XR did not increase the $^{238}UH^+$ formation although a Jet sampler cone with larger orifice diameter was used. Kim et al. have investigated the influence of the interference effect of ^{238}U at 239 *m/z* with various sample introduction systems, and found that the MCN-6000 microconcentric nebulizer coupled with the membrane desolvation system showed the lowest hydride formation [27], while the MicroMist and Q-DiHEN systems showed a much higher interference effect from the formation of $^{238}UH^+$ [28]. As shown in Table 2, the $^{238}UH^+$ formation rate obtained with the APEX-Q and Aridus II systems in Element XR was comparable with that of the MCN-6000 sample introduction system, and was among the lowest values reported in the literature. In previous studies, the author and co-workers developed a highly effective chemical separation method for Pu determination in environmental samples with extremely high U decontamination factor (10^6 for soil and sediment, 10^7-10^8 for seawater) [22,29]. Therefore, the influences of uranium hydride molecular ions, as well as the peak tailing effect from ^{238}U were considered negligible for the determination of Pu isotopes in environmental samples when combining the highly sensitive SF-ICP-MS with the developed chemical separation methods.

3.3. Precision and accuracy of Pu isotope ratio measurement. The precision (RSD %) and accuracy of Pu isotope analysis using the Aridus II/SF-ICP-MS (with Jet Interface) system were estimated by a single measurement (runs × passes 20 × 4) of 100 fg mL^{-1} ^{239}Pu (NBS 947 Pu isotope standard solution), and compared with the values obtained with the Element XR without using the Jet Interface (Table 3). The Element XR without the Jet Interface gave a precision of the $^{240}Pu/^{239}Pu$ atom ratio of 20.5 % and accuracy of -3.3 %, and the Aridus II/SF-ICP-MS (with Jet Interface) gave a precision of 5.0 % and accuracy of 0.83 %; both precision and accuracy were significantly improved for the latter.

Figure 4 shows the effect of Pu concentrations (^{239}Pu and ^{240}Pu) on the precision, based on a single measurement (runs × passes 20 × 4) using the APEX-Q/SF-ICP-MS (Element XR). The concentrations of Pu investigated were 1, 5, 10, 20, 50 and 110 fg mL^{-1} for ^{239}Pu and 0.24, 1.21, 2.65, 4.82, 12.1 and 26.5 fg mL^{-1} for ^{240}Pu. For $^{240}Pu/^{239}Pu$ atom ratio, the RSD % varied from 7 % to 45 %, it decreased with Pu concentration increase. Better RSD % values lower than 10 % could be obtained when ^{240}Pu was higher than 4.82 fg mL^{-1}.

It is necessary to check how reliable the isotopic ratio measurement with the instrument for a long-term. Thus the long-term stability of the SF-ICP-MS (Element XR) for the determination of $^{240}Pu/^{239}Pu$ atom ratio at ultra-trace level was estimated from April to December 2014, an 8-month period, using the APEX-Q/SF-ICP-MS system with NBS 947 at a concentration level of 11 fg mL^{-1} ^{239}Pu and 2.7 fg mL^{-1} ^{240}Pu. As shown in Figure 5, during eight months, the variation of the detected $^{240}Pu/^{239}Pu$ atom ratios was within ±1σ, indicating excellent long-term stability for ultra-trace level Pu isotope analysis.

3.4. Determination of Pu isotopes in sediment and seaweed reference materials. Two standard reference materials,

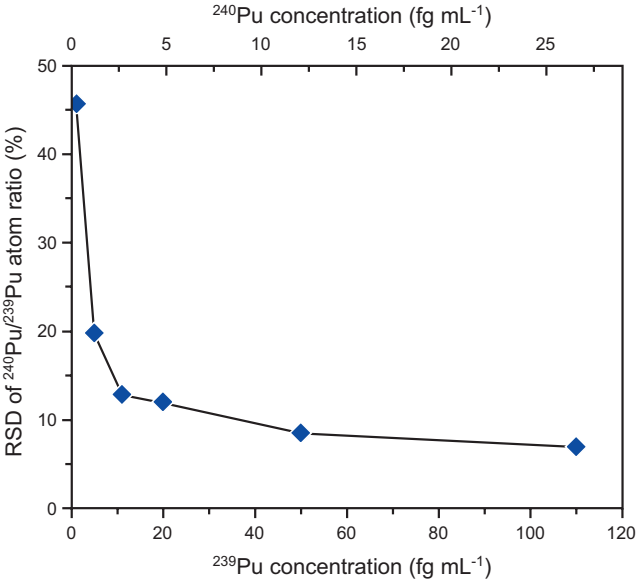

Figure 4. Relative standard deviation (RSD %) for the $^{240}Pu/^{239}Pu$ atom ratio in NBS-947 measured by the APEX-Q/SF-ICP-MS plotted against ^{239}Pu and ^{240}Pu concentrations.

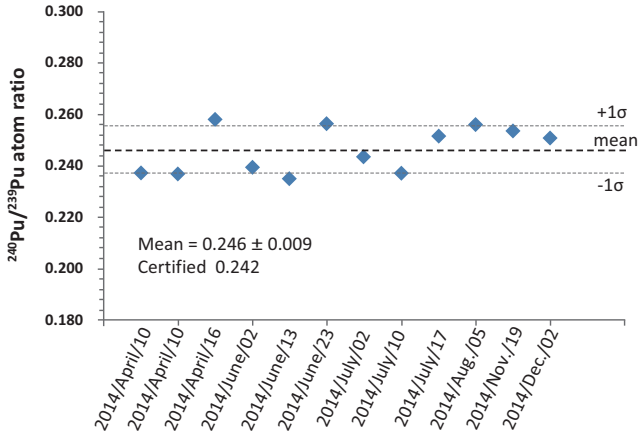

Figure 5. Long-term (8 month) stability of the APEX-Q/SF-ICP-MS (Element XR) for the determination of $^{240}Pu/^{239}Pu$ atom ratios of NBS-947 (11 fg mL^{-1} ^{239}Pu and 2.7 fg mL^{-1} ^{240}Pu).

NIST-4357 ocean sediment and IAEA-446 seaweed were analyzed for Pu isotopes. The results we obtained are compared with the certified and previously reported values [22, 30-33]. Table 4 summarized the analytical results of activities of $^{239+240}Pu$ and ^{241}Pu, and atom ratios of $^{240}Pu/^{239}Pu$ and $^{241}Pu/^{239}Pu$. As can be seen, the mean $^{239+249}Pu$ activities for NIST-4357 (n = 5) and IAEA-446 (n = 3) were 10.82 ± 1.39 and 0.026 ± 0.001 mBq g^{-1}, respectively, agreed well with the certified values. In addition, for IAEA-446, the mean (n = 3) of $^{240}Pu/^{239}Pu$ atom ratio was 0.222 ± 0.003, also agreed well with the certified value of 0.220 ± 0.006 [33]. For NIST-4357, we also measured ^{241}Pu activity and $^{241}Pu/^{239}Pu$ atom ratio. Although the atom ratios of $^{240}Pu/^{239}Pu$ and $^{241}Pu/^{239}Pu$, and the activity of ^{241}Pu were not certified for NIST-4357, they were reported in the literature [22, 30-33]. In this study, the mean (n = 5) atom ratios of $^{240}Pu/^{239}Pu$ and $^{241}Pu/^{239}Pu$, and the activity of ^{241}Pu were 0.238 ± 0.002, 0.0130 ± 0.0006, and 124.1 ± 14.9 mBq g^{-1}, respectively, which were comparable with the literature values. These results demonstrated the applicability of the new SF-ICP-MS equipped with the Jet Interface for ultra-trace determination of Pu isotopes in environmental samples. Currently, this new analytical system has been applied to the determination of Pu isotopes in various environmental samples, such as sediment, seawater, soil and agricultural crops for radiological impact assessment following the Fukushima Daiichi Nuclear Power Plant accident.

4. Conclusions

In this study a detail evaluation was made on the analytical potential of a new SF-ICP-MS equipped with the Jet Interface for ultra-trace determination of Pu isotopes. In order to further improve the sensitivity for Pu isotope analysis, high efficiency sample introduction systems (APEX-Q and Aridus II) were combined with the new SF-ICP-MS. A certified Pu isotope standard solution (NBS-947) and a U standard solution (Merck

TABLE 4: Results of reference materials measured in this study using APEX-Q/SF-ICP-MS and the certified and information values

Sample	Amount (g)	$^{239+240}Pu$ activity (mBq g^{-1})[a]	^{241}Pu activity (mBq g^{-1})[a,c]	$^{240}Pu/^{239}Pu$ atom ratio[a]	$^{241}Pu/^{239}Pu$ atom ratio[a,c]
NIST-4357 1	0.538	9.36±0.48	115.6±11.6	0.239±0.009	0.0140±0.0045
NIST-4357 2	0.525	12.34±0.93	139.8±16.4	0.238±0.005	0.0129±0.0036
NIST-4357 3	0.530	10.24±0.70	115.1±15.1	0.241±0.008	0.0128±0.0050
NIST-4357 4	0.619	9.87±0.44	109.3±9.3	0.236±0.008	0.0125±0.0042
NIST-4357 5	0.608	12.26±0.30	140.6±13.9	0.238±0.008	0.0128±0.0040
mean (n=5)[b]		**10.82±1.39**	**124.1±14.9**	**0.238±0.002**	**0.0130±0.0006**
IAEA-446 1	7.813	0.025±0.003		0.219±0.028	
IAEA-446 2	3.829	0.026±0.005		0.222±0.041	
IAEA-446 3	3.267	0.027±0.005		0.225±0.048	
mean (n=3)[b]		**0.026±0.001**		**0.222±0.003**	
Certified/information values					
NIST-4357		9.2-13.3	119.5±13.3[d]	0.233-0.244[e]	0.0132±0.0007[f]
IAEA-446		0.022-0.026		0.220±0.006[g]	

[a]Uncertainties represent 1σ error; [b]Average of the measured replicates ± standard deviation.[c] Decay of ^{241}Pu corrected to 1 Jan. 2000; [d]Data cited from Bu et al. [22]; [e]Data cited from Hrnecek et al. [30] and Yoshida et al. [31]; [f]Data cited from Zhang et al. [32]; [g]Data cited from Pham et al. [33].

multi element standard) were used to investigate four items: the formation rate of $^{238}UH^{+}$, which could interfere with ultra-trace level ^{239}Pu determination; the detection limit for Pu; the precision and accuracy for $^{240}Pu/^{239}Pu$ atom ratio determination; and the long-term (8-month) stability for Pu isotope composition analysis. For a single measurement (runs × passes 20 × 4), the precision of the $^{240}Pu/^{239}Pu$ atom ratio lower than 10 % could be obtained with a concentration level of 11 fg mL^{-1} ^{239}Pu and 2.7 fg mL^{-1} ^{240}Pu. Due to the exceptional sensitivity of the new SF-ICP-MS, a detection limit at the attogram (10^{-18} g) level was achieved, which was comparable or even surpass that of AMS.

Acknowledgements

The author wishes to acknowledge Dr. K. Tagami, Dr. S. Uchida, Dr. Z. T. Wang, Mr. W. T. Bu and Mr. L. G. Cao for their useful discussion and constructive suggestions. This work was supported by the Agency for Natural Resources and Energy (METI), Japan.

References

(1) M. E. Ketterer and S. C. Szechenyi, Spectrochim. Acta B **63**, 719 (2008).
(2) Y. Muramatsu, W. Ruhm, S. Yoshida, K. Tagami, S. Uchida and E. Wirth, Environ. Sci. Technol. **34**, 2913 (2000).
(3) J. Zheng, K. Tagami, Y. Watanabe, S. Uchida,T. Aono, N. Ishii, S. Yoshida, Y. Kubata, S. Fuma, and S. Ihara, Sci. Rep. **2**: 304, doi:10.1038/srep00304 (2012).
(4) D. M. Taylor, Environmental plutonium-creation of the universe to twenty-first century mankind, in A. Kudo (Ed.), Plutonium in the environment. Elsevier, Amsterdam, pp. 1 (2001).
(5) J. Qiao, X. Hou, M. Miro and P. Roos, Anal. Chim. Acta **652**, 66 (2009).
(6) J. Zheng, K. Tagami, and S. Uchida, Environ. Sci. Technol. **47**, 9584 (2013).
(7) P. Borretzen, W. J. F. Standring, D. H. Oughton, M. Dowdall, L. K. Fifield, Environ. Sci. Technol. **39**, 92 (2005).
(8) J. Zheng, K. Tagami, S. Homma-Takeda and W. T. Bu, J. Anal. At. Spectrom. **28**, 1676 (2013).
(9) K. J. Moody, I. D. Hutcheon, and P. M. Grant, Nuclear Forensic Analysis. CRC Press, Boca Raton, FL. (2005).
(10) D. L. Donohue, Strengthening IAEA safeguards through environmental sampling and analysis. J. Alloys Compd. **271-273**, 11 (1998).
(11) F. C. Wu, J. Zheng, H. Q. Liao and M. Yamada, Environ. Sci. Technol. **44**, 2911 (2010).
(12) J. Zheng, F. C. Wu, M. Yamada, H. Q. Liao, C. Q. Liu and G. J. Wan, Environ. Pollut. **152**, 314 (2008).
(13) Y. Igarashi, Y. Inomata, M. Aoyama, K. Hirose, H. Takahashi, Y. Shinoda, N. Sugimoto, A. Shimizu and M. Chiba, Atmos. Environ. **43**, 2971 (2009).
(14) M. E. Ketterer, K. M. Hafer and J. W., Mietelskj, J. Environ. Radioact. **73**, 183 (2004).
(15) K. Hirose, Y. Igarashi, M. Aoyama, C. K. Kim, C. S. Kim, and B. W. Chang, J. Environ. Monit. **5**, 302 (2003).
(16) M. V. Zoriy, C. Pickhardt, P. Ostapczuk, R. Hille, and J. S. Becker, Int. J. Mass Spectrom. 232, 217 (2004).
(17) D. Schaumloffel, P. Giusti, M. V. Zoriy, C. Pickhardt, J. Szpunar, R. Yobinski, and J. S. Becker, J. Anal. At. Spectrom. **20**, 17 (2005).
(18) J. Zheng and M. Yamada, Talanta **69**, 1246 (2006).
(19) P. Lindahl, M. Keith-Roach, P. Worsford, M. S. Choi, H. S. Shin, and S. H. Lee, Anal. Chim. Acta **671**, 61 (2010).
(20) http://www.thermoscientific.jp/content/dam/tfs/ATG/CMD/CMD%20Documents/BR-30027-ELEMENT-2-and-ELEMENT-XR-Brochure.pdf
(21) J. W. H. Lam, and G. Horlick, Spectrochim. Acta B **45**, 1313 (1990).
(22) W. T. Bu, J. Zheng, Q. J. Guo, T. Aono, H. Tazoe, K. Tagami, S. Uchida, and M. Yamada, Environ. Sci. Technol. **48**, 534 (2014).
(23) S. Olivier, S. Bajo, L. K. Fifield, H. W. Gäggeler, T. Papina, P. H. Santschi, U. Schotterer, M. Schwikowski and L. Wacker, Environ. Sci. Technol. **38**, 6507 (2004).
(24) X. L. Zhao, W. E. Kieser, X. Dai, N. D. Priest, S. Kramer-Tremblay, J. Eliades, and A. E. Litherland, Nucl. Instrum. Methods Phys. Res. B **294**, 356 (2013).
(25) X. Dai, M. Christl, S. Kramer-Tremblay, and H. A. Synal, J. Anal. At. Spectrom. **27**, 126 (2012).
(26) L. Skipperud, and D. H. Oughton, Environ. Int. **30**, 815 (2004).
(27) C. S. Kim, C. K. Kim, J. I. Lee, K. J. Lee, J. Anal. At. Spectrom. **15**, 247 (2000).
(28) J. S. Becker, J. Anal. At. Spectrom. **17**, 1172 (2002).
(29) W. T. Bu, J. Zheng, Q. J. Guo, T. Aono, K. Tagami, S. Uchida, H. Tazoe, and M. Yamada, J. Chromatogr. A. **1337**, 171 (2014).
(30) E. Hrnecek, R. Jakopic, A. Wallner, and P. A. Steier, J. Radioanal. Nucl. Chem. **276**, 789 (2008).
(31) S. Yoshida, Y. Muramatsu, S. Yamazaki, and T. Ban-nai, J. Environ. Radioact. **96**, 85 (2007).
(32) Y. Zhang, J. Zheng, M. Yamada, F. Wu, Y. Igarashi, and K. Hirose, Sci. Total Environ. **408**, 1139 (2010).
(33) M. K. Pham, M. Benmansour, F. P. Carvalho, E. Chamizo, D. Degering, C. Engeler, C. Gasco, J. P. Gwynn, A. V. Harms, E. Hrnecek, F. L. Ibanez, C. IIchmann, T. Ikaheimonen, G. kanisch, M. Kloster, M. Llaurado, A. Mauring, B. Moller, T. Morimoto, S. P. Nielsen, H. Nies, L.D.R. Norrlid, H. B. L. Pettersson, P. P. Povinec, U. Rieth, C. Samuelsson, J. Schikowski, B. V. Silobritiene, P. A. Smedley, M. Suplinska, V. P. Vartti, E. Vasileva, J. Wong, T. Zalewska, and W. Zhou. Appl.Radiat. Isot. **87**, 468 (2014).